Hindawi Publishing Corporation
Research Letters in Materials Science
Volume 2008, Article ID 206019, 5 pages
doi:10.1155/2008/206019

Research Letter

Surface and Interface Properties of 10–12 Unit Cells Thick Sputter Deposited Epitaxial CeO_2 Films

L. V. Saraf, C. M. Wang, M. H. Engelhard, and P. Nachimuthu

Environmental Molecular Sciences Laboratory, Pacific Northwest National Laboratory, Richland WA 99352, USA

Correspondence should be addressed to L. V. Saraf, lax.saraf@pnl.gov

Received 11 March 2008; Accepted 8 May 2008

Recommended by William A. Jesser

Ultrathin and continuous epitaxial films with relaxed lattice strain can potentially maintain more of its bulk physical and chemical properties and are useful as buffer layers. We study surface, interface, and microstructural properties of ultrathin (∼10–12 unit cells thick) epitaxial ceria films grown on single crystal YSZ substrates. The out-of -plane and in-plane lattice parameters indicate relaxation in the continuous film due to misfit dislocations seen by high-resolution transmission electron microscopy (HRTEM) and substrate roughness of ∼1-2 unit cells, confirmed by atomic force microscopy and HRTEM. A combination of secondary sputtering, lattice mismatch, substrate roughness, and surface reduction creating secondary phase was likely the cause of surface roughness which should be reduced to a minimum level for effective use of it as buffer layers.

Copyright © 2008 L. V. Saraf et al. This is an open access article distributed under the Creative Commons Attribution License, which permits unrestricted use, distribution, and reproduction in any medium, provided the original work is properly cited.

1. INTRODUCTION

Cerium oxide is a widely studied material across several disciplines due to its use in oxygen storage, catalysis, and solid oxide fuel cells [1–3]. Epitaxial cerium oxide layers also act as buffer layers for metal oxide semiconductors (MOS-s), silicon on insulator (SOI) for ferroelectrics, and superconducting thin films. It has a cubic fluorite structure that is very stable in a broad temperature and pressure range. The reversible oxygen storage, oxygen diffusion, surface desorption, electrical conductivity of ceria are widely studied by us and others in the catalysis community [2, 4–7]. Doping ceria with +3 valence elements creates oxygen vacancy which can be an electrolyte for solid oxide fuel cells with oxygen ion conductivity in the intermediate temperature range [3]. It has been shown that growth of epitaxial ceria on silicon can create metal oxide emiconductor (MOS) layers useful in electronics [8]. Due to good lattice and thermal expansion coefficient matching with c-oriented epitaxial yttrium barium copper oxide (YBCO) superconductors, ceria had been consistently studied as a buffer layer to grow superconductors [9, 10]. The buffer layers have also been shown to create proximity effect in superconductors [11]. Because strained films can undergo structural phase transition modifying its physical and chemical properties, it may become essential to minimize the changes in physical and chemical properties of ultrathin ceria buffer layers while maintaining its overall continuous and epitaxial/oriented nature.

Due to nearly matching lattice parameters, similar cubic structures and thermal expansion coefficients for ceria and yttrium stabilized zirconia (YSZ), epitaxial growth of ceria on YSZ was demonstrated by us [12, 13]. In general, techniques like molecular-beam epitaxy or atomic layer deposition have been utilized to grow epitaxial films [14]. Especially, when ultrathin layer depositions are critical, these techniques have good control over the film growth parameters. Reactive oxide DC sputtering on the other hand has other advantages like compatibility with semiconductor processes, higher growth rates, a high degree of ionization of evaporated species, and the ability to grow on relatively large areas [14]. There have been some reports discussing ultrathin ceria films less than 5 nm in thickness grown by sputtering [15, 16]. One of the major challenges of this technique is to avoid secondary sputtering from the surface of already deposited films. Since the binding energies of most of the solids are on the order of few electron volts, for films with few unit cell in thickness, minor changes in incident ion energy can lead to variation in secondary sputtering rate from the film surfaces which can cause morphology changes resulting

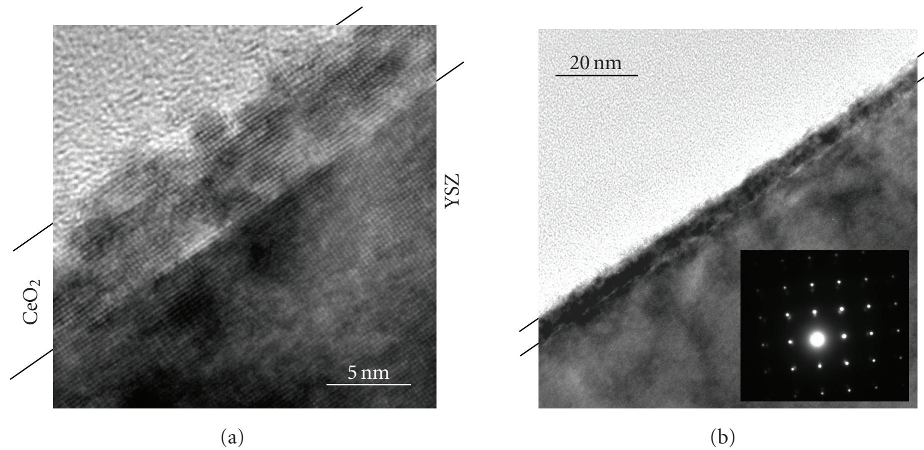

Figure 1: HRTEM and TEM micrographs of 10–12 unit cell thick epitaxial ceria film grown on single crystal YSZ.

in increased roughness. Different types of thin film growth modes are modeled and reviewed by Gilmer et al. [17]. In this report, we discuss surface and interface properties of 10–12 unit cell thick epitaxial ceria film with the film surface roughness in the range of 1-2 unit cells. Defects in the form of misfit dislocations cause relaxation in ceria films. A combination of secondary sputtering, lattice mismatch, substrate roughness, and secondary phase at the surface were most likely responsible for the film surface roughness.

2. EXPERIMENT

DC magnetron sputtering was used to grow cerium oxide thin films on YSZ. A cerium metal target was sputtered in a (1 : 1) mixture of argon and oxygen gases. The (001) oriented single-crystal YSZ substrates were sequentially cleaned in acetone, methanol, and water using an ultrasonic bath. In the growth chamber, the cerium target and YSZ substrate were kept approximately 8 inches apart. The total sputter power was kept at 100 Watts to avoid formation of particulates on the substrates. A 10–15-minute presputtering was carried out to clean the target surface. The films were grown on YSZ substrates at 750°C and 12 mbar total $Ar+O_2$ pressure. After deposition, the substrates were cooled at a rate of 5°C/min. More importantly, sputtering time with a growth blocking shutter was used to control film thickness. In the present case, 10–12 unit cells thick ceria films were achieved after sputtering for 1 minute.

High-resolution X-ray diffraction (XRD) and measurements were carried out on a Phillips X'pert θ-2θ diffractometer. Jade 6.0 software from Materials Data Inc. was used to facilitate the fitting of the X-ray profile scans. X-ray reflectivity (XRR) measurements were carried out using a Philips X'Pert multipurpose diffractometer. The thickness, roughness, and density of the films were determined from the fitting of XRR data by BEDE REFS V4.00 code. The a-axis parameter of the YSZ substrate was measured at 0.5143 nm. For the calculation purposes, bulk lattice parameter of ceria was used 0.541 nm [5–7, 12, 13]. A Digital Instruments Nanoscope IIIa Multimode microscope was utilized for atomic force microscopy (AFM) analysis using a tapping mode. In the case of low- and high-resolution transmission electron microscopy (HRTEM) measurements, a standard tripod wedge polishing method followed by Ar-ion-beam thinning was used to obtain an electron transparent sample. HRTEM analysis was carried out on a JEOL 2010 microscope with a lateral resolution of 0.194 nm. The digital recording of the images was captured using a CCD camera (1024 × 1024 pixels) followed by processing with digital micrograph. XPS measurements were carried out using a physical electronics quantum 2000 scanning ESCA microprobe. A focused monochromatic Al Kα X-rays (1486.7 eV) source with 16-element multichannel detection was used in the experiment. The X-ray beam was a 101 W, 107 μm diameter beam which was scanned over an area of 1.4 mm × 0.2 mm. The high-energy resolution data was collected using pass energy of 23.5 eV. The binding energy scale was calibrated by setting Cu $2p_{3/2}$ position at 932.6 eV and Au $4f_{7/2}$ position at 83.9 eV.

3. RESULTS AND DISCUSSION

Figures 1(a) and 1(b) represent HRTEM and TEM micrographs of ceria thin film grown on YSZ single crystal. A good cube-on-cube epitaxy can be seen in the HRTEM image (Figure 1(a)). Good film coverage and the overall uniformity of the layer can be seen in Figure 1(b). A diffraction pattern is shown as inset of Figure 1(b), where film and substrate reflections related to (h 0 0) family of planes are evident indicating epitaxial growth. The Fourier transformation of HRTEM image (Figure 1(a)) is shown in Figure 2. The misfit dislocations, indicated by arrows in film and substrate and ellipses (in the interface region), can be seen in the image. XRR and AFM measurements on ceria thin film are shown in Figures 3(a) and 3(b), respectively. Fitting of the XRR profile indicates that the thickness of the ceria films is 6 nm which is in good agreement with TEM images shown in Figure 1. The inset of Figure 3(a) is the XRD scan, where no other orientations than (200) and (400) are observed. The AFM image in Figure 3(b) shows the surface morphology of 6 nm thick ceria film. The root-mean-square roughness

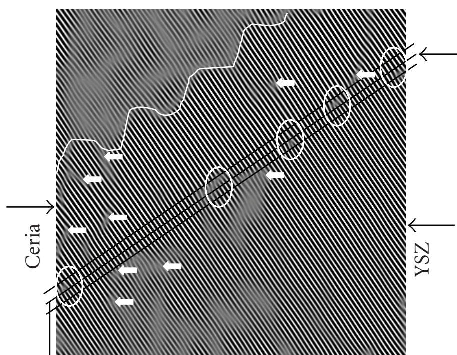

Figure 2: The Fourier transformation of 10–12 unit cell thick ceria film. The misfit dislocations, indicated by arrows and ellipses.

was calculated to be 0.3 nm for the 500 nm × 500 nm scan area using a silicon cantilever with a nominal tip radius of curvature of 10 nm. Since this represents average roughness, HRTEM image indicates surface roughness variation around 1-2 unit cells (up to ∼1 nm). The inset of Figure 3(b) shows an AFM image of commercially as-received YSZ single-crystal substrate used in the present study, after a typical cleaning cycle mentioned above. Step-like features ∼100 nm wide and several nanodots were observed on the substrates. A significant size distribution of nanodots indicates that these features may have been resulted from the crystal polishing process. In one of the previous studies, these nanodots on as-received YSZ single crystal substrates were also connected to the atomic scale irregularities resulting from point defects. [18] That study also observes that after annealing at 1250°C resulted in removal of much of these nanodots with an ordering in step-like features.

To determine out-of-plane and in-plane lattice constants of ceria thin films, slow HRXRD measurements were carried out for (200) and (420) planes. The data are shown in Figures 4(a) and 4(b). We have calculated that c- (out-of-plane) and a-axis (in-plane) lattice constants were 0.539 nm and 0.54 nm, respectively, indicating negligible strain. The visualization of (200) and (420) planes in ceria lattice are shown as the insets to Figures 4(a) and 4(b). The difference in the broadness of ceria and YSZ peaks in this figure clearly highlights the difference between the bulk and the ultrathin nature of these layers. Figure 5 shows XPS spectrum collected at 20° emission angle from a typical epitaxial ceria film grown on YSZ single crystal [19]. At this emission angle, the data is mostly independent of the film thickness more than 5 nm. Low emission angle XPS provides information about ceria surface states due to enhanced signal from roughly first ∼5 nm. We observed that even though the bulk film indicates epitaxial ceria (Ce^{4+}) film, as shown in inset XRD spectrum of Figure 5, surface has the presence of Ce^{3+} valence state. The results point toward reduction in ceria with a possibility of phase separation at the surface. Since surface roughness and phase separation are mutually dependent factors, phase separation is likely a major contributing factor for ceria surface roughness [20].

Ideally, a critical thickness can be achieved in every epitaxial film, where lattice mismatch gets accommodated in

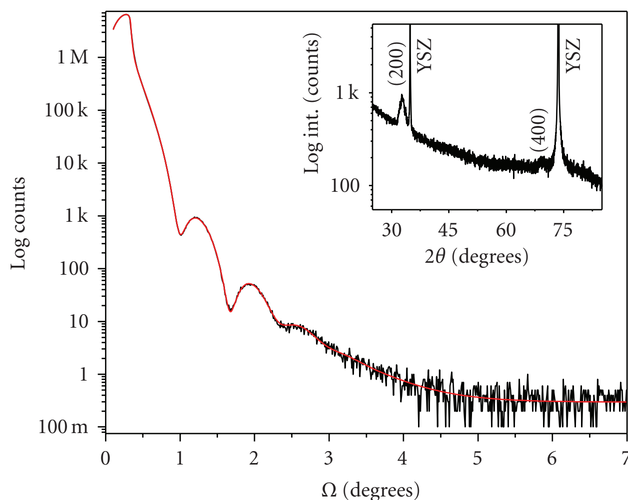

(a)

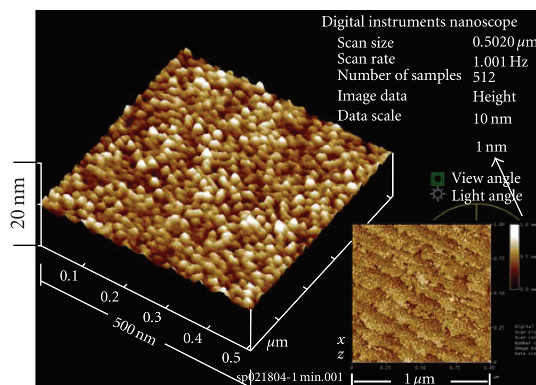

(b)

Figure 3: (a) XRR and (b) AFM measurements on 10–12 unit cell thick epitaxial ceria film. Insets of (a) and (b) represent an XRD scan and AFM image of the as-received YSZ substrate, respectively.

the form of a uniform strain [21]. Above such thicknesses, a misfit dislocation is an energetically favored process. In the case of ceria/YSZ pair, we have observed a critical thickness ∼64 nm [12]. Several extrinsic experimental factors such as gas flow rates, their mixing ratios and substrate temperatures can also affect this parameter. A combination of XRD peak broadening, peak position shifts, and analysis of HRTEM images by Fourier transformation can give some information about the nature of strains and misfit dislocations. Minor c and a axis strains indicate relaxation of ceria films due to misfit dislocations observed in Fourier transformed HRTEM image. In a recent report, similar lattice parameter values were obtained at these thicknesses when the films were grown on hexagonal r-plane Al_2O_3, where lattice mismatch is even greater [15]. In that case, no full film coverage was obtained until ceria thickness reaches 8 nm. A “lattice constant”-“oxygen incorporation” relationship was also discussed suggesting that at extremely low-thicknesses ceria may

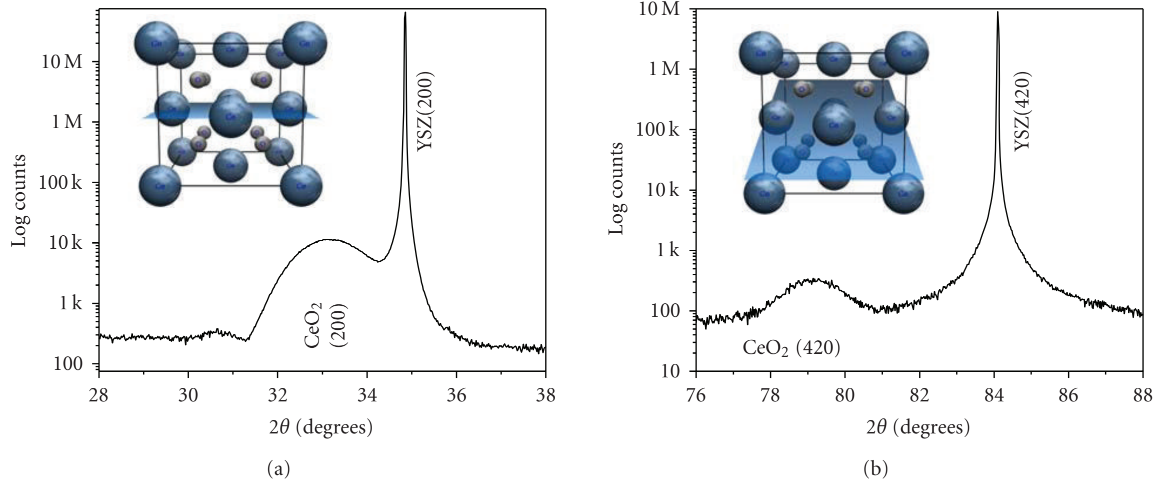

FIGURE 4: (a) Out-of-plane (200) and (b) in-plane (420) XRD scans of 10–12 unit cell thick ceria film, necessary to calculate the respective lattice parameters. The insets indicate visualization of (200) and (420) planes in a ceria lattice.

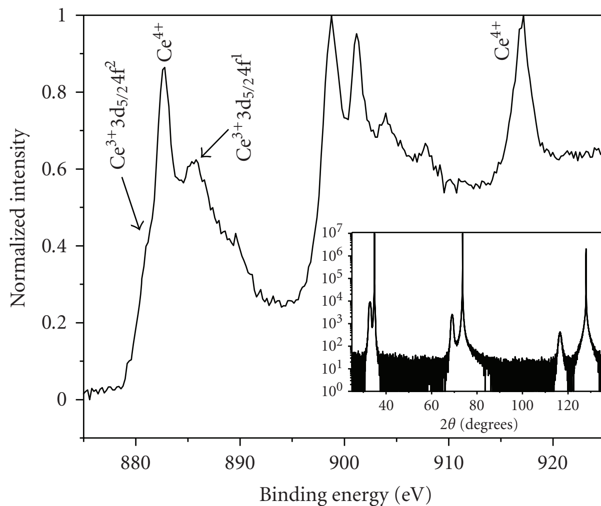

FIGURE 5: XPS Ce 3d photoemission spectrum of a typical epitaxial CeO_2/YSZ film when the data is collected at emission angles of 20°. Inset: XRD scan of the same film.

not be fully oxidized. This phenomenon may enhance the lattice parameters by as much as 3.7% in ultrathin epitaxial ceria films [15]. This argument combined with XPS result indicates that there is some oxygen deficiency at the surface if we consider Ce^{3+} state from a CeO_2 oxygen deficient form and near complete oxidation of the state if it is from Ce_2O_3 like features.

Ceria-YSZ combination has low lattice mismatch of ~5% [YSZ (a-0.514 nm) and ceria (a-0.541 nm)] and nearly matching thermal expansion coefficients from room temperature to around the present growth temperature range [22]. Even though misfit dislocations, as seen in Fourier transformed HRTEM image in Figure 2 relax majority of strain, effects of substrate lattice mismatch on film surface roughness can not be completely ruled out. Generally, the substrate coverage during the growth of ultrathin epitaxial films rapidly changes during initial growth stages. High surface mobility of the deposited atoms can be achieved with the help of relatively high growth temperatures. Several types of thin film growth modes such as layer by layer and nucleation followed by islands formations are discussed in the literature [17]. The techniques like XRR and AFM can be effectively utilized to measure surface roughness. In our case, an rms roughness of 0.3 nm roughly represents an average thickness variation less than c-axis of a ceria unit cell. When we compare it to the overall thickness, it is about 5% of the total thickness. By taking into account the lack of atomic layer manipulation capability in sputter process, given roughness is in an acceptable range. Additionally, when we consider as-received substrate roughness, surface-phase separation, and secondary sputtering, these roughness parameters can be further justified.

4. CONCLUSION

We have studied surface and interface properties of 10–12 unit cell thick epitaxial ceria films grown on single crystal YSZ substrates by DC magnetron sputtering. An average roughness of ~0.3 nm or about 5% of the total film thickness with roughness variation in the range of 1-2 unit cells was observed. The relaxation in epitaxial ceria is caused by lattice misfit dislocations. Because the surface of typical epitaxial ceria has Ce^{3+} valence state, major factors contributing the surface roughness were single-crystal substrate roughness, lattice mismatch, the secondary sputtering caused by the sputter process, and phase separation at the ceria surface. Minimizing all of these parameters can more help to establish better control over the process and effective use of ceria as buffer layers.

ACKNOWLEDGMENTS

The authors would like to thank D. E. McCready, A. S. Lea, V. Shutthanandan, and S. Thevuthasan for help in XRD measurements and discussions. This work was done

in Environmental Molecular Sciences Laboratory (EMSL) at Pacific Northwest National Laboratory (PNNL). PNNL is operated by Battelle for the US Department of Energy. EMSL is a national scientific user facility for the Office of Biological and Environmental Research (BER). The support for this work is provided by BER under the contract DE-AC06-76RLO1830.

REFERENCES

[1] M. S. Dresselhaus and I. L. Thomas, "Alternative energy technologies," *Nature*, vol. 414, no. 6861, pp. 332–337, 2001.

[2] N. V. Skorodumova, S. I. Simak, B. I. Lundqvist, I. A. Abrikosov, and B. Johansson, "Quantum origin of the oxygen storage capability of ceria," *Physical Review Letters*, vol. 89, no. 16, Article ID 166601, 4 pages, 2002.

[3] B. C. H. Steele and A. Heinzel, "Materials for fuel-cell technologies," *Nature*, vol. 414, no. 6861, pp. 345–352, 2001.

[4] C. L. Perkins, M. A. Henderson, C. H. F. Peden, and G. S. Herman, "Self-diffusion in ceria," *Journal of Vacuum Science & Technology A*, vol. 19, no. 4, pp. 1942–1946, 2001.

[5] L. V. Saraf, V. Shutthanandan, Y. Zhang, et al., "Distinguishability of oxygen desorption from the surface region with mobility dominant effects in nanocrystalline ceria films," *Journal of Applied Physics*, vol. 96, no. 10, pp. 5756–5760, 2004.

[6] L. V. Saraf, C. M. Wang, V. Shutthanandan, et al., "Oxygen transport studies in nanocrystalline ceria films," *Journal of Materials Research*, vol. 20, no. 5, pp. 1295–1299, 2005.

[7] L. V. Saraf, D. W. Matson, V. Shutthanandan, C. M. Wang, O. Marina, and S. Thevuthasan, "Growth of YSZ columnar nanostructures with CeO_2 impingement," *Electrochemical and Solid-State Letters*, vol. 8, no. 10, pp. A525–A527, 2005.

[8] M. Suzuki and T. Ami, "A proposal of epitaxial oxide thin film structures for future oxide electronics," *Materials Science & Engineering B*, vol. 41, no. 1, pp. 166–173, 1996.

[9] Y. Yamada, T. Muroga, H. Iwai, T. Watanabe, S. Miyata, and Y. Shiohara, "Progress of PLD and IBAD processes for YBCO wire in the SRL-Nagoya coated conductor centre—new method for a coated conductor using a *self-epitaxial* PLD-CeO_2 buffer," *Superconductor Science and Technology*, vol. 17, no. 2, pp. S70–S73, 2004.

[10] M. S. Bhuiyan, M. Paranthaman, S. Sathyamurthy, et al., "MOD approach for the growth of epitaxial CeO_2 buffer layers on biaxially textured Ni-W substrates for YBCO coated conductors," *Superconductor Science and Technology*, vol. 16, no. 11, pp. 1305–1309, 2003.

[11] F. Tafuri and J. R. Kirtley, "Weak links in high critical temperature superconductors," *Reports on Progress in Physics*, vol. 68, no. 11, pp. 2573–2663, 2005.

[12] L. V. Saraf, D. E. McCready, V. Shutthanandan, C. M. Wang, M. H. Engelhard, and S. Thevuthasan, "Correlation among channeling, morphological and micro-structural properties in epitaxial CeO_2 films," *Electrochemical and Solid-State Letters*, vol. 9, no. 5, pp. J17–J20, 2006.

[13] C. M. Wang, S. Azad, V. Shutthanandan, et al., "Microstructure of ZrO_2-CeO_2 hetero-multi-layer films grown on YSZ substrate," *Acta Materialia*, vol. 53, no. 7, pp. 1921–1929, 2005.

[14] P. R. Willmott, "Deposition of complex multielemental thin films," *Progress in Surface Science*, vol. 76, no. 6–8, pp. 163–217, 2004.

[15] G. Linker, R. Smithey, J. Geerk, F. Ratzel, R. Schneider, and A. Zaitsev, "The growth of ultra-thin epitaxial CeO_2 films on r-plane sapphire," *Thin Solid Films*, vol. 471, no. 1-2, pp. 320–327, 2005.

[16] T. Inoue, N. Sakamoto, M. Ohashi, S. Shida, A. Horikawa, and Y. Sampei, "Orientation selective epitaxial growth of CeO_2(100) and CeO_2(110) layers on Si(100) substrates," *Journal of Vacuum Science & Technology A*, vol. 22, no. 1, pp. 46–48, 2004.

[17] G. H. Gilmer, H. Huang, and C. Roland, "Thin film deposition: fundamentals and modeling," *Computational Materials Science*, vol. 12, no. 4, pp. 354–380, 1998.

[18] G. Kuri, M. Gupta, R. Schelldorfer, and D. Gavillet, "Diffusion behaviour of Nb in yttria-stabilized zirconia single crystals: a SIMS, AFM and X-ray reflectometry investigations," *Applied Surface Science*, vol. 253, no. 3, pp. 1071–1080, 2006.

[19] K. T. Koch and L. V. Saraf, "Synthesis and characterization of pure and doped ceria films by sol-gel and sputtering," *Journal of Undergraduate Research*, vol. 4, pp. 84–90, 2004.

[20] I.-K. Park, Y.-S. Kim, M.-K. Kwon, et al., "Surface roughness induced phase-separation in InGaN and LED applications," *Physica Status Solidi C*, vol. 2, no. 7, pp. 2887–2890, 2005.

[21] J. H. van der Merwe, "Crystal interfaces—part I: semi-infinite crystals," *Journal of Applied Physics*, vol. 34, no. 1, pp. 117–122, 1963.

[22] Y. Du, N. M. Sammes, G. A. Tompsett, D. Zhang, J. Swan, and M. Bowden, "Extruded tubular strontium- and magnesium-doped lanthanum gallate, gadolinium-doped ceria, and yttria-stabilized zirconia electrolytes: mechanical and thermal properties," *Journal of the Electrochemical Society*, vol. 150, no. 1, pp. A74–A78, 2003.

Journal of
Nanotechnology

International Journal of
Corrosion

International Journal of
Polymer Science
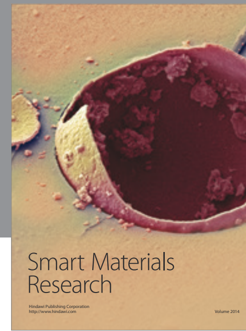
Smart Materials
Research

Journal of
Composites

BioMed
Research International

Hindawi
Submit your manuscripts at
http://www.hindawi.com
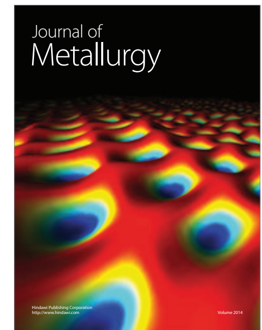
Journal of
Metallurgy

Journal of
Materials
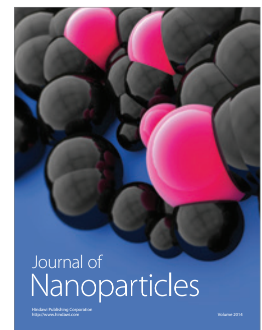
Journal of
Nanoparticles
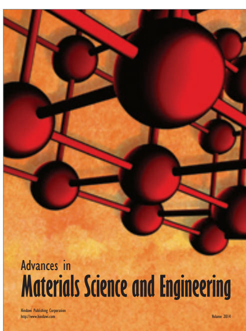
Advances in
Materials Science and Engineering

Scientifica
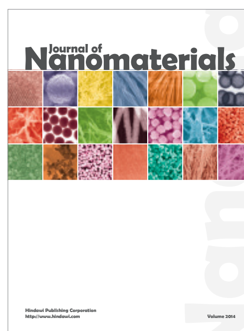
Journal of
Nanomaterials
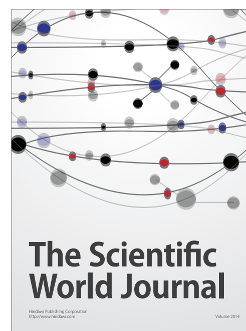
The Scientific
World Journal
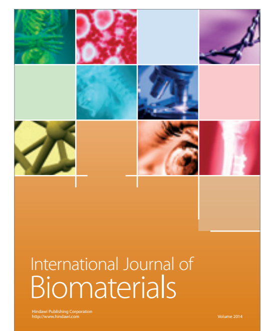
International Journal of
Biomaterials

Journal of
Nanoscience

Journal of
Coatings

Journal of
Crystallography

Journal of
Ceramics
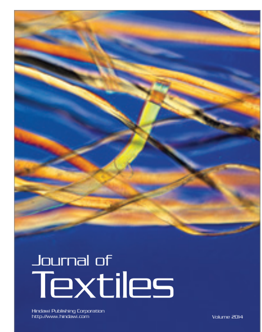
Journal of
Textiles